

# From Unimodal to Multimodal: improving the sEMG-Based Pattern Recognition via deep generative models

Wentao Wei, Linyan Ren

**Abstract**—Multimodal hand gesture recognition (HGR) systems can achieve higher recognition accuracy. However, acquiring multimodal gesture recognition data typically requires users to wear additional sensors, thereby increasing hardware costs. This paper proposes a novel generative approach to improve Surface Electromyography (sEMG)-based HGR accuracy via virtual Inertial Measurement Unit (IMU) signals. Specifically, we trained a deep generative model based on the intrinsic correlation between forearm sEMG signals and forearm IMU signals to generate virtual forearm IMU signals from the input forearm sEMG signals at first. Subsequently, the sEMG signals and virtual IMU signals were fed into a multimodal Convolutional Neural Network (CNN) model for gesture recognition. To evaluate the performance of the proposed approach, we conducted experiments on 6 databases, including 5 publicly available databases and our collected database comprising 28 subjects performing 38 gestures, containing both sEMG and IMU data. The results show that our proposed approach outperforms the sEMG-based unimodal HGR method (with increases of 2.15%-13.10%). It demonstrates that incorporating virtual IMU signals, generated by deep generative models, can significantly enhance the accuracy of sEMG-based HGR. The proposed approach represents a successful attempt to transition from unimodal HGR to multimodal HGR without additional sensor hardware.

**Index Terms**—Muscle-computer interface, hand gesture recognition, deep generative model, virtual acceleration signals, unimodal to multimodal.

## I. INTRODUCTION

Pattern recognition is a pivotal technology of achieving natural and intuitive Human-Computer Interaction (HCI). It

converts the user's movements into commands for device control and interface manipulation. Surface Electromyography (sEMG) is a bioelectric signal generated during skeletal muscle contraction, which collected by myoelectric electrodes placed on the skin [1]. The sEMG can be indicative of human movement intention, even when collected from the residual limb of amputees [2]. Therefore, sEMG-based pattern recognition systems are widely utilized. The sEMG-based HCI, which is also known as a Muscle-Computer Interface (MCI) [3], has shown great potential in many fields such as prosthesis control [4, 5], rehabilitation engineering [6, 7], virtual reality [8, 9], and human-computer interaction [10, 11].

A critical aspect of creating a seamless and efficient MCI relies on precise pattern recognition. Deep learning (DL) methods have been demonstrated the superior performance in improving the accuracy of sEMG-based pattern recognition [12, 13]. However, these approaches are of low interpretability because the DL-based gesture recognition process is being considered as a “black-box” for myoelectric control, thereby making further improvement of recognition accuracy challenging [14, 15]. The accuracy of sEMG-based pattern recognition systems in recognizing gestures composed of hand and forearm movements remains limited. This can be attributed to 1) the forearm muscles such as the anterior flexors, the posterior extensors, the lateral extensor-supinators, and the medial flexor-pronators mainly control the movement of the wrist and fingers, thus the forearm sEMG signals provide limited information for recognition of complex gestures containing forearm movements [16, 17]; 2) sEMG signals are non-stationary stochastic signal with a high signal-to-noise ratio, such inherent nature can predictably affect the outcomes of gesture recognition [18]. Multimodal HGR has been proposed as an explainable promising approach [19, 20].

The authors are with the School of Design Arts and Media, Nanjing University of Science and Technology, Nanjing 210094, China. (Wentao Wei and Linyan Ren are co-first authors.) (Corresponding author: Wentao Wei. e-mail: [weiwentao@njust.edu.cn](mailto:weiwentao@njust.edu.cn))

Multimodal HGR involves input data streams from at least two modalities that can provide more information for HGR from different dimensions. The multimodal combination of incorporating Inertial Measurement Unit (IMU) signals as an additional information source to sEMG signals is widely recognized [21, 22]. Because the sEMG is an intuitive biosignal that can contribute to capturing subtle differences in similar hand gesture while the IMU signals is good at capturing hand orientations and hand and forearm movements [23, 24]. However, for MCIs, sEMG-IMU-based multimodal HGR systems require additional IMU sensors, which increases the hardware cost [25]. Therefore, how to implement multimodal HGR without additional sensor hardware is of great significance for low-cost human-computer interaction system.

Deep generative models such as Generative Adversarial Networks (GAN) are able to generate high-dimensional and complex data by learning the intrinsic correlation and latent distribution of the training data [26, 27]. Many of the currently available sEMG benchmark databases, such as the subdatabases of NinaPro, provide synchronously captured forearm IMU signals data [28-32]. By exploring the intrinsic correlation between sEMG signals and IMU signals of performed gestures and training a deep generative model, it becomes feasible to generate corresponding virtual forearm IMU signals from the input forearm sEMG signals, thus achieving multimodal HGR systems that use sEMG signals and generated virtual IMU signals as inputs.

The major contributions of our work are as follows:

- We propose a novel generative multimodal HGR approach based on generative learning, which can bridge the gap between the unimodal HGR and multimodal HGR without additional sensor hardware.
- We train a deep generative model based on the intrinsic correlation between forearm sEMG signals and IMU signals, and then generate virtual forearm IMU signals by feeding sEMG signals into the trained deep generative model.
- Experimental results from three publicly available databases and our collected database demonstrate that incorporating virtual IMU signals can significantly improve the accuracy of sEMG-based HGR.

The remainder of this paper is organized as follows. Section II reviews the related work; section III formulates the generative multimodal learning problems; section IV introduces the details of the proposed approach; section V demonstrates the experimental results; section VI concludes the paper and discusses future work.

## II. RELATED WORKS

In recent years, significant advancements have been made in the performance of sEMG-based unimodal HGR systems through various approaches such as manually constructing more effective feature sets [1, 33] and training advanced deep learning models with higher performance [34, 35]. As sEMG is a high-noise, non-stationary random signal, previous research typically extracted hand-crafted features from the sEMG signals for gesture recognition rather than directly using the raw sEMG signals. Feature extraction is used to highlight positive information in the sEMG signal and diminishes the influence of noise and negative sEMG signals [1]. The time-domain (TD), frequency-domain (FD), or time-frequency-domain (TFD) features are manually extracted from the raw sEMG signal [20, 36]. However, the accuracy of HGR is directly affected by the validity of the selected features.

With the increase of sEMG databases and the development of deep neural network technology, an increasing number of researchers are focusing on deep learning-based sEMG HGR methods [37, 38]. Compared to traditional shallow learning models, the main advantage of deep learning is its strong feature learning ability, which enables automatic feature learning and the construction of end-to-end sEMG HGR systems without relying on manual feature extraction and selection processes [1]. Deep learning models, such as CNNs, have demonstrated superior performance in the sEMG-based HGR system. For instance, Shen et al [39] designed a CNN-based model for sEMG signal gesture classification, which outperformed Linear Discriminant Analysis (LDA), Support Vector Machine (SVM), and Random Forests on the Ninapro DB5 database by 5.02%, 6.61%, and 5.47% in accuracy, respectively. Inspired by the success of CNNs in image classification, feature learning approaches based on CNN have been extensively explored in HD-sEMG-based HGR and shown promising results, that is, surpassing 95.00% accuracy [38, 39]. However, experimental results on large-

scale multichannel databases show that the performance of these unimodal (sEMG signals only) HGR systems based on the deep learning models is still limited in recognizing gestures composed of hand and forearm movements. For example, Geng et al. [40] proposed an end-to-end CNN model (i.e. GengNet) which achieved a gesture recognition accuracy of 99.60% using HD-sEMG but reached only 77.80% accuracy with sparse multichannel sEMG. Notably, a pioneering novel Convolutional Vision Transformer (CvT) with stacking ensemble learning proposed by Shen et al. [41] achieved gesture recognition accuracies of 80.02% (with a 200 ms window length) on the NinaPro DB2 and 76.83% and 73.23% on Exercise A and Exercise B of NinaPro DB5, respectively. Additionally, many existing deep learning models are regarded as black-box models, making it difficult for us to ascertain the specific mechanisms responsible for improving gesture recognition accuracy [20, 42, 43]. This making further improvement of sEMG-based unimodal HGR accuracy challenging.

The advancement of hardware technology has enabled an increasing number of human-computer interaction devices to support multimodal perception. Newly emerging myoelectric human-machine interface products such as the CTRL-labs armband [44] and eCon armband [45] have integrated sEMG electrodes and IMU to support simultaneous sensing of sEMG signals and motion sensing signals. Previous studies have shown that multimodal HGR can achieve higher recognition accuracy in recognizing gestures composed of hand and forearm movements. Take the NinaPro database as an example, which include basic finger movements as well as wrist, grasp and functional movements performed by the hand and forearm. Duan et al. [21] proposed a novel and practical sEMG-ACC-based hybrid fusion (HyFusion) model, and achieved high accuracy of 94.73%, 89.60%, and 96.44% on the NinaPro DB2, DB3, and DB7, respectively. Shen et al. [46] proposed a flexible and modular method based on sEMG and ACC signals, and recognition accuracy on 49 hand gestures (NinaPro DB2) is 94.24%, much higher than the accuracy of the method only using sEMG signals.

Typically, multimodal HGR requires additional sensor hardware for acquiring another modal signal, which increases hardware cost. Deep generative models are designed to generate new data instances that are indistinguishable from the real data [47]. As a powerful tool

for generating complex data, deep generative models such as GAN [27] and its variants [48-50], Variational Autoencoder (VAE) [51], Diffusion Model [52] are widely used in the fields of image synthesis [53-55], natural language processing[56] and audio generation [57, 58]. Based on the properties of the generative model, we try to train a GAN-based generative model to generate virtual forearm IMU signals rather than directly collecting forearm IMU signals using additional sensors in this work.

Gesture recognition based on hand movements fundamentally involves recognizing hand postures. To improve the accuracy of sEMG-based HGR, a novel hybrid approach that combines real sEMG signals with corresponding virtual hand poses was proposed by Hu et al [25], resulting in an accuracy improvement of 5.2% on the sparse multichannel sEMG databases. However, the hand poses mainly reflect the subtle motion of the finger and do not provide information about the forearm posture, thus resulting in limited accuracy improvement in recognizing gestures composed of hand and forearm movements [59]. IMU signals present a viable option as they can offer information hand orientations and hand and forearm movements [23, 24]. Moreover, the hand poses include a relatively large number of channels (22-channel), which increases the complexity of the model [28, 29]. It is worth noting that IMU signals contain different types of signals with different numbers of channels, such as ACC signals (36-channel or 3-channel in this work) and Euler angle signals (3-channel in this work). Researchers can select the appropriate IMU signals based on their specific needs and device configurations. Motivated by this, we present a novel deep generative multimodal HGR approach in this paper. Our aim is to improve the accuracy of sEMG-based HGR with generative virtual IMU signals, which can implement multimodal HGR without additional sensor hardware.

### III. PROBLEM STATEMENT

The problem of sEMG-IMU-based multimodal gesture recognition can be formulate as:

$$\mathcal{Z} = H(m_{sEMG}, m_{imu}; \theta) \quad (1)$$

where  $\mathcal{Z}$  represents classification results,  $H$  is the multimodal gesture recognition model used to process the sEMG signals  $m_{sEMG}$  and IMU signals  $m_{imu}$ ,  $\theta$  is the

parameter of  $H$ . To achieve multimodal HGR without additional sensor hardware, virtual forearm IMU signals  $m_{v\_imu}$  instead of real forearm IMU signals were used in this work, see (2).

$$z = H(m_{sEMG}, m_{v\_imu}; \theta) \quad (2)$$

The problem of sEMG-based HGR by generative multimodal approach can be divided into two parts. Firstly, we train a deep generative model to generate virtual forearm IMU signals based on the corresponding input forearm sEMG signals. Then, we train a multimodal CNN for sEMG-virtual IMU-based multimodal PR.

#### A. Deep generative model for multimodal signal generation

As mentioned above, the deep generative model in this paper is built based on GAN. GAN-based deep generative model consists of a generator  $G$  and a discriminator  $D$ , as shown in Fig. 1. Given a segment of an forearm sEMG signals of  $k$  frames (denoted by  $m_{sEMG} = [s_1, s_2, \dots, s_k | s_i \in R^{C_1}]$ , where  $C_1$  is the number of sEMG signal channel), the generator  $G$  takes the forearm sEMG signals  $m_{sEMG}$  as input and outputs the

virtual forearm IMU signals (denoted by  $m_{v\_imu} = [a'_1, a'_2, \dots, a'_k | a'_i \in R^{C_2}]$ , where  $C_2$  is the number of IMU signal channel), see (3).

$$m_{v\_imu} = G(m_{sEMG}; \theta_g) \quad (3)$$

where  $m_{v\_imu}$  is the virtual forearm IMU signals,  $G$  is the generative model used to generate virtual forearm IMU signals  $m_{v\_imu}$  from the input forearm sEMG signals  $m_{sEMG}$ ,  $\theta_g$  is the parameter of  $G$ .

The discriminator  $D$  is a binary classifier that takes real IMU signals  $m_{imu}$  and generated virtual IMU signals  $m_{v\_imu}$  as inputs  $m$ , and outputs the probability distribution  $D(m)$  of samples coming from real rather than generated ones. The generator  $G$  and discriminator  $D$  alternate in an adversarial fashion during training. Specifically, the generator  $G$  aims to produce more realistic data, while the discriminator  $D$  attempts to better distinguish between real and generated data. The objective function in training is shown in Eq. (4), and the optimization goal is to achieve Nash equilibrium [60], at which point the generator model  $G$  is believed to have captured the distribution of real samples [61].

$$\min_G \max_D V(D, G) = E_{x \sim P_t(m_{imu})} [\log D(x)] + E_{y \sim P_t(m_{sEMG})} [\log(1 - D(G(y)))] \quad (4)$$

where  $D(x)$  denotes the probability that the discriminator  $D$  judges the input data  $x$  as a real sample,  $x$  is the data from the real IMU signal distribution  $P_t(m_{imu})$ ;  $D(G(y))$  denotes the probability that the discriminator

$D$  judges that the generated sample  $G(y)$  as a real sample,  $y$  is the data from the sEMG signal distribution  $P_t(m_{sEMG})$ .

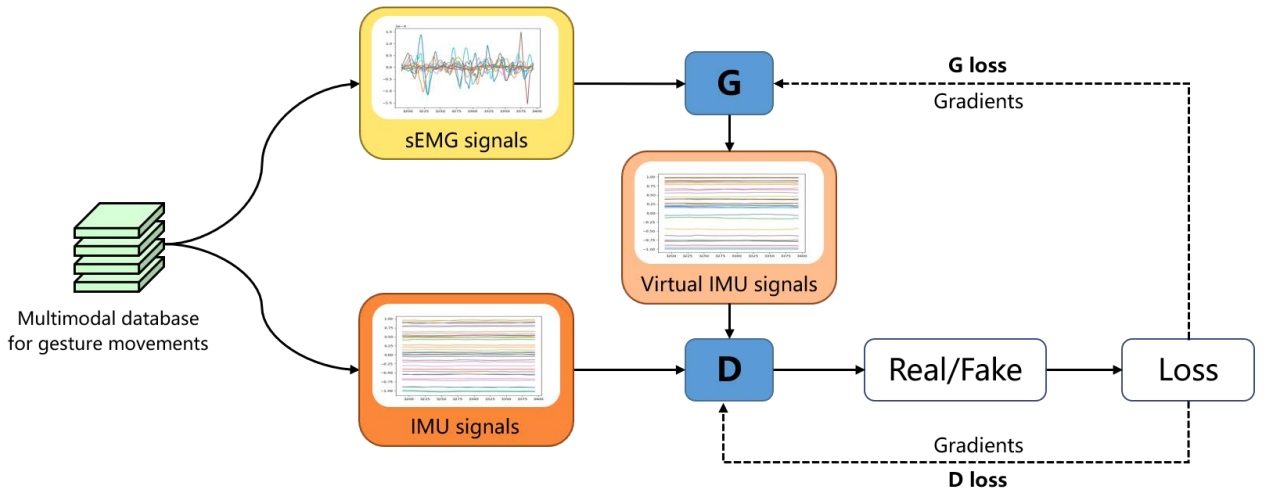


Fig. 1. Illustration of proposed GAN-based deep generative model

### B. Multimodal CNN for multimodal PR

Multimodal HGR necessitates the concurrent input of multiple modal signals, for instance, sEMG signals and virtual IMU signals. Thereby, a multimodal CNN model need requires multiple branches to accommodate these signals, and then output the classification result through the integrated fusion of these branches. This multimodal HGR process can be formulated as follows:

$$z = H_f(H_s(m_{sEMG}; \theta_s), H_i(m_{v\_imu}; \theta_i); \theta_f) \quad (5)$$

where  $z$  represents classification results in form of output softmax scores from the multimodal CNN,  $H_s$  is the CNN branch used to process the forearm sEMG

signals  $m_{sEMG}$ ,  $\theta_s$  is the parameter of  $H_s$ ,  $H_i$  is the CNN branch used to process the virtual forearm IMU signals  $m_{v\_imu}$ ,  $\theta_i$  is the parameter of  $H_i$ ,  $H_f$  is the fusion model that fuses multiple CNN branches,  $\theta_f$  is the parameter of  $H_f$ .

### IV. PROPOSED APPROACH

The proposed generative multimodal HGR approach is implemented using a generative multimodal model, which includes the GAN-based deep generative model and multimodal CNN model, as shown in Fig. 2.

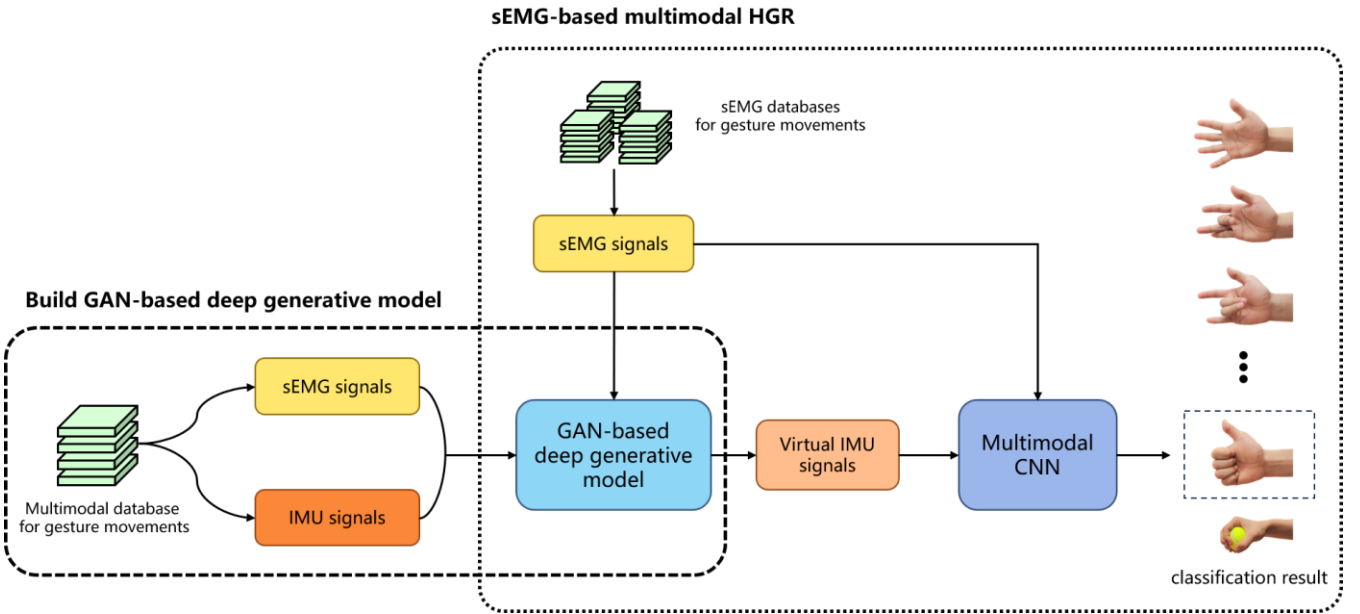


Fig. 2. Illustration of proposed generative approach

### A. GAN-based deep generative model

The neural network structure of proposed GAN-based deep generative model is shown in Fig. 3. We utilized Deep Convolutional Generative Adversarial Networks (DCGAN) to generate virtual forearm IMU signals from the input forearm sEMG signals in this work. DCGAN is a powerful deep generative model proposed by Radford et al. in 2015 [49], which is a variant of Generative Adversarial Networks (GAN). Compared with the GAN, the DCGAN model improves the quality of generated samples and the convergence speed by replacing the original nonlinear maps with convolutional layers and transposed convolution layers [62].

As shown in Fig. 3, the generator  $G$  consists of three

transposed 2D convolutional layers and one fully connected (FC) layer. Three transposed 2D convolutional layers consist of 32, 16 and 1  $3 \times 3$  filters with a stride of (1, 2), respectively. The output sEMG signal features are then flattened and fed into a FC layer, with a number of neurons equivalent to the desired number of virtual IMU signals to be generated. Batch Normalization (BN) [63] and ReLU nonlinearity function [64] are applied to each transposed convolutional layer, and tanh activation function is applied to the FC layer.

The discriminator  $D$  consists of one 2D convolutional layers and one FC layer. The convolutional layers consist of 16  $3 \times 3$  filters with a stride of 2. The output

sEMG signal features are then flattened and fed into a FC layer, which consist of 1 hidden unit. The BN and LeakyReLU activation function [65] are applied to the

convolutional layer, and dropout [66] is applied to prevent overfitting. The Sigmoid is used as the activation function on the FC layer, i.e., the output layer.

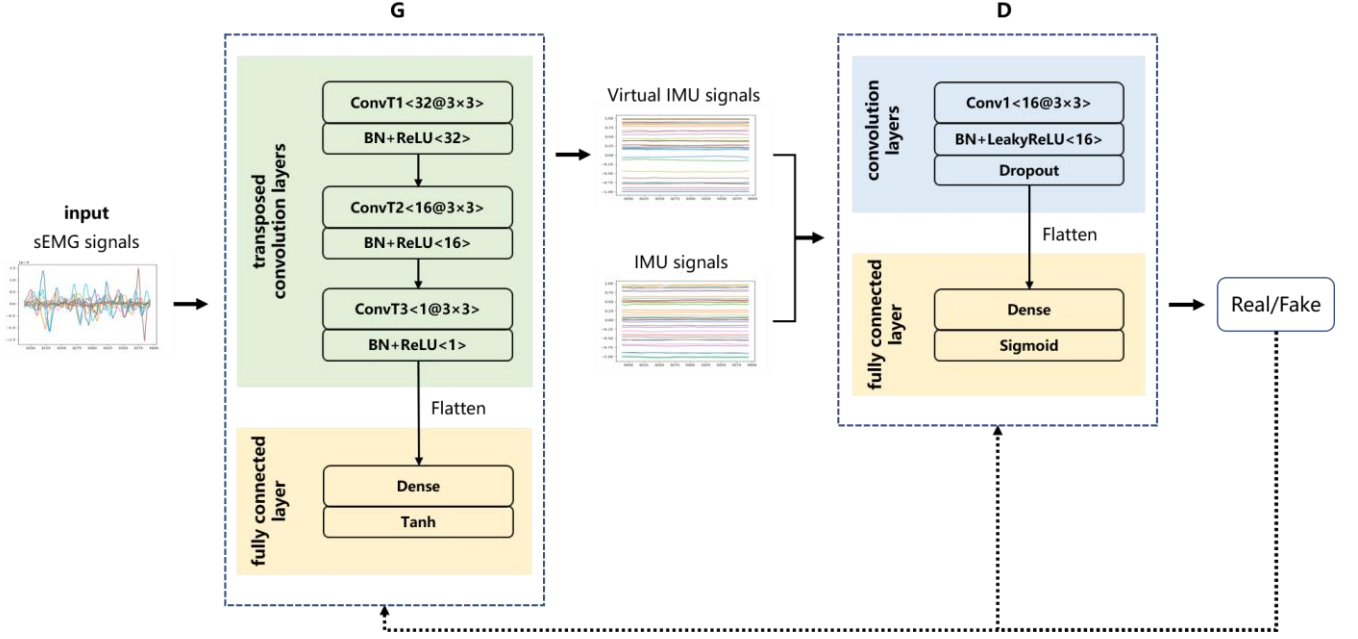


Fig. 3. Illustration of neural network structure of proposed GAN-based deep generative model

### B. Multimodal CNN

The proposed multimodal CNN presented in this work is a dual-stream CNN that used sEMG and virtual IMU as its multimodal signal inputs. As illustrated in Fig. 4, each stream of the CNN comprises two convolutional layers, one locally connected (LC) layer, and one fully connected (FC) layer. Each convolutional layer is composed of 64  $3 \times 3$  filters with a stride of 1, the LC layer is composed of 64  $1 \times 1$  filters with a stride of 1. Subsequently, the outputs from each CNN stream are flattened and separately input into an FC layer with 512 hidden units. Studies have shown that the LC layer imposes an inductive bias by constraining certain features to only appear in specific regions of the input space [67], with filters do not share weights [68]. Compared to the convolution layer, the LC layer has better learning capabilities for local features in images. In order to accelerate the training process and improve

convergence speed, the BN and ReLU nonlinearity function are applied to the convolutional layers and LC layers [63, 64]. Additionally, the BN is added before the first convolutional layer in each CNN stream, and dropout is applied to the last FC layer to prevent overfitting.

The outputs of these multiple CNNs are then fused to obtain the final classification results. The fusion module comprises two FC layers. Initially, the output feature vectors from each CNN stream are concatenated and input into an FC layer with 512 hidden units. The ReLU nonlinearity functions is added preceding the FC layer, while BN and ReLU nonlinearity functions are applied following the FC layer. Subsequently, a G-way FC layer with softmax activation is used to obtain the classification results, where G represents the number of gesture categories.



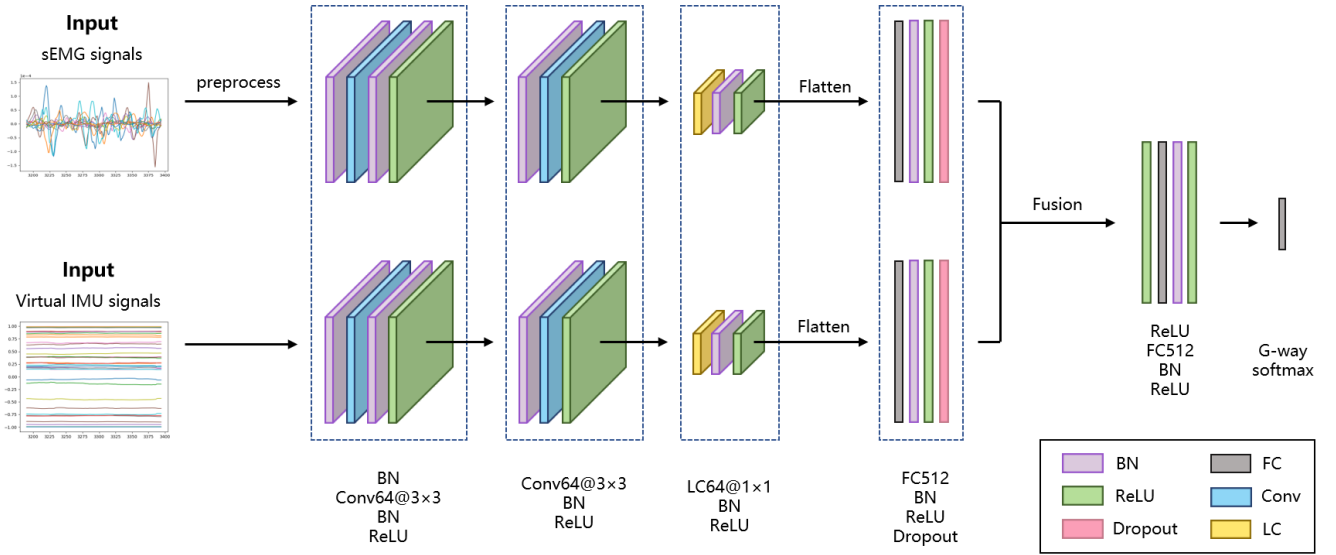


Fig. 4. Illustration of neural network structure of proposed multimodal CNN

## V. EXPERIMENTS AND RESULTS

In our work, the experiments are divided into two parts. First, the HGR performance of the proposed generative multimodal HGR approach is compared with the unimodal HGR approach that uses only sEMG as input. Second, we conduct a performance comparison with

state-of-the-art methods. Six databases utilized for model training and evaluation in this work include our collected database and 5 publicly available databases (4 subdatabases of the NinaPro database and SIEM database). The specifications of the databases can be found in Table I.

TABLE I  
SPECIFICATIONS OF THE DATABASES USED IN THIS PAPER

Name	Intact subjects	Amputated subjects	Number of subjects to be classified	Number of gestures to be classified	Number of sEMG channels	Number of IMU channels		Number of trials	Number of trials to be classified	Sampling rate
						ACC	Euler			
FEMG-VPF Database	28	0	28	38	8	—	3	6	4	2040Hz
NinaPro DB2 [28]	40	0	40	50	12	36	—	6	6	2000Hz
NinaPro DB3 [28]	0	11	6	50	12	36	—	6	6	2000Hz
NinaPro DB5 [29]	10	0	10	53	16	3	—	6	6	200Hz
NinaPro DB7 [30]	20	2	20	41	12	36	—	6	6	2000Hz
SIEM Database [69]	20	0	20	12	8	—	3	18	6	2040Hz

### A. Data acquisition

To validate the performance of our proposed approach in recognizing gestures composed of hand and forearm movements, we created own database, named “ForeArmEMG-VariedPosForce”, denoted as “FEMG-VPF” database. The FEMG-VPF database contains the 18 hand gestures and one rest gesture under two distinct forearm states. Below is a detailed description of the database and its data acquisition process.

1) *Subjects*: The FEMG-VPF database contains data obtained from 28 intact subjects (16 males and 12 females, with an age range of  $23.00 \pm 2.83$  years, 26

right-handed and 2 left-handed). More details about the subjects are reported in Table II. All subjects had no known skeletal and/or neuromuscular disorders with no previous myoelectric control experience. The subjects were recruited from the Nanjing University of Science and Technology in China. A brief description of the experimental setup and goals was provided to potential individuals, and those who expressed interest was provided further details and then scheduled to have a data acquisition session. All subjects were given a full verbal description of the methods, purposes, and protocols for the experiments. Each subject read and signed an informed consent form before proceeding with

the experiments. All the procedures were performed in accordance with the Declaration of Helsinki and relevant policies in China.

2) *Data acquisition setup*: The sEMG signals and Euler angles in the IMU signals of the forearm muscles were recorded (at a sampling rate of 200Hz and an A/D resolution of 8 bits) by a Myo armband (Talmic Labs, Canada), which is a commercial myoelectric armband with eight bipolar dry-electrode channels [69]. This Myo armband device uses high accuracy zero drift micropower operational amplifiers (TSZ124, STMicroelectronics) with a CMRR of 115 dB and a GBP of 400 kHz. Notably, the FEMG-VPF database also includes forearm HD-sEMG signals collected with a portable sEMG amplifier (Sessantaquattro, OT Bioelectronica, Italy) with 64-channel HD-sEMG electrode grid (OT Bioelectronica, Italy) placed on the forearm surface, sampled at a rate of 2040Hz. The HD-sEMG and sparse multichannel sEMG were recorded synchronously, hence, the sEMG signals from the Myo armband were recorded at a synchronous rate 2040Hz. The data collection process both Myo armband and HD-sEMG is completely non-invasive, thus it does not cause any discomfort or harm to the subjects [70, 71]. To ensure a high correlation between the sEMG and Euler angles used in this study, we exclusively used the sparse multichannel sEMG signal and corresponding Euler angles in the IMU signals gathered by the Myo armband. Despite the relatively lower sampling rate and number of channels, the Myo armband exhibits a comparable HGR accuracy to other devices, as reported by Pizzolato et al. [29]. In addition, several previous studies have demonstrated the effectiveness of the MYO armband in gesture recognition applications [72, 73].

Each subject was comfortably seated on a chair with a straight back and relaxed shoulders in front of a 40-inch LCD monitor on which the experiment information was displayed. This information included stimuli (the finger movements the subject needs to make) and multiple types of relevant data (such as the average HD-sEMG, the HD-sEMG activation map, and the sEMG data of the Myo armband). The data acquisition was controlled by a laptop through a self-developed Qt Program. The two acquisition devices had independent threads, and batches of data from the two devices were synchronized and

fetched from the random access memory (RAM) of the computer. The raw data acquisition was conducted using a PC running 64-bit Microsoft Windows 10 with an Intel i7 1.73-GHz processor, and an 8-GB RAM.

3) *Data acquisition procedure*: The FEMG-VPF database encompasses 38 gestures composed of hand and forearm movements. The hand gestures were performed under two distinct arm postures: 1) the upper arm naturally drooping with the forearm parallel to the ground, and 2) the upper arm naturally drooping with the forearm at a 45-degree angle to the ground. Each arm posture incorporates one resting gesture (i.e. 0 rest gesture), 15 finger movements (i.e. 1-15) and 3 grasping gestures (i.e. 16-18). Detailed descriptions of the hand gestures and the arm postures are shown in Fig. 5(a) and Fig. 5(b), respectively. The finger movements encompassed in the database include single-finger movement, double-finger movement, triple-finger movement, and full-hand movements. The grasping gestures incorporate actions grasping cylindrical objects (i.e., mineral water bottles), planar objects (i.e., books), and spherical objects (i.e., tennis balls), respectively. Each gesture was performed 6 repeated trials, namely four high-force trials and two low-force trials. Give that the effect of incorporating virtual IMU signals on the gesture recognition accuracy is considered in this work, we utilized the data solely from four high-force trials to mitigating the impact of force variation on the outcomes. The subjects were instructed to first complete all gestures in the 0° arm posture before proceeding with those in the 45° arm posture, and always start and finish trials in the resting position (with the arm posture fixed and the fingers relaxed). The acquisition time of each trial is 6 seconds. Rest for the first 1 seconds, then start gesturing. As shown in Fig. 6, a 3-second action gesture and a 0.5-second rest gesture were selected to represent stable static gestures in this work. Subsequently, the rest gesture signals from the 18 action gestures in each arm posture were extracted and spliced, totaling 9 seconds. Each subject had a break after completing every six gestures, and also was allowed to have rest at any other time [69]. Our FEMG-VPF database is now publicly available for research purposes, and interested researchers can access the database through the Figshare data repository [74].



TABLE II  
SPECIFICATIONS OF THE SUBJECTS IN FEMG-VPF DATABASES

Subject	Age	Gender	Height (cm)	Weight (kg)	Forearm Circumference (cm)	Laterality	Subject	Age	Gender	Height (cm)	Weight (kg)	Forearm Circumference (cm)	Laterality
S01	25	Male	176	75	27.5	Right	S15	24	Female	160	70	25	Right
S02	24	Male	179	74	28	Right	S16	21	Female	160	56	24	Right
S03	24	Male	178	64.5	25.2	Right	S17	21	Female	171	75	24	Right
S04	31	Male	170	63	25	Right	S18	21	Female	163	56	23	Right
S05	31	Male	178.5	63	22.5	Right	S19	21	Female	164	65	25.5	Right
S06	24	Male	180	88	34	Right	S20	21	Female	158	60	19	Right
S07	21	Male	176	70	24.5	Right	S21	22	Female	164	70	23.4	Right
S08	21	Male	182	70	23.4	Right	S22	19	Female	168	58	21.8	Right
S09	22	Male	181	81	23.5	Right	S23	23	Female	168	70	24	Right
S10	21	Male	179	75	26	Right	S24	23	Female	158	57	28	Right
S11	20	Male	178	57	22.7	Right	S25	24	Female	172	66	24	Right
S12	20	Male	173	59	22.5	Right	S26	25	Male	178	69	24.5	Right
S13	21	Male	183	83	24.2	Left	S27	24	Male	165	69	26	Left
S14	24	Female	169	59.5	22	Right	S28	26	Male	174	66	24	Right

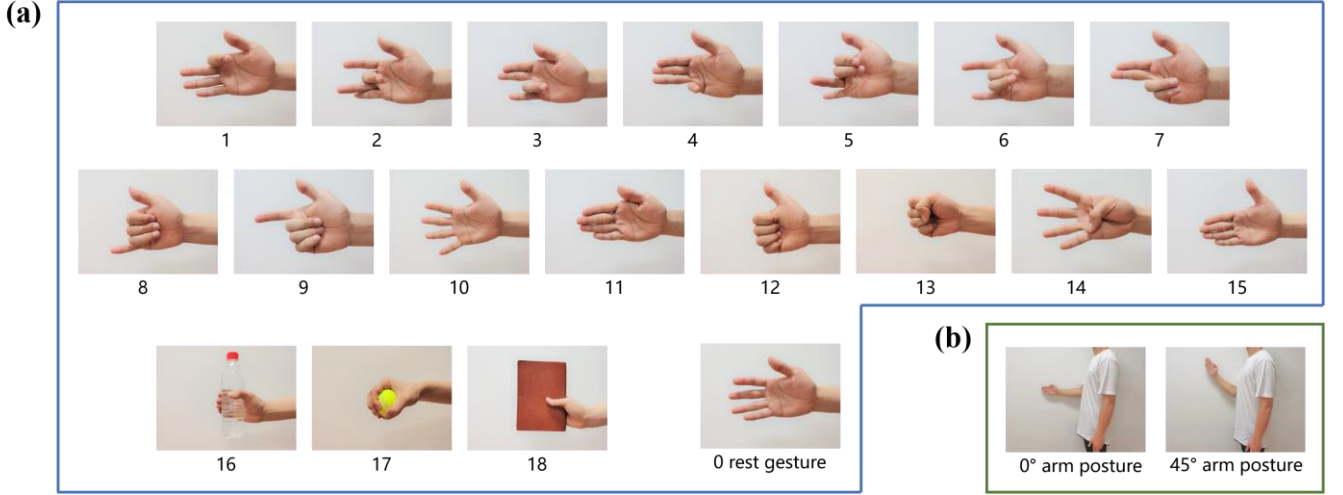


Fig. 5. The specification of the FEMG-VPF database. (a) Images of the 18 hand gestures and the rest gesture. (b) Images of two arm postures



Fig. 6. The movement trajectory and selected gesture data of each trial in this work

### B. Publicly available databases

1) *NinaPro database*: The NinaPro database is a publicly available large-scale gesture movement benchmark database that include various categories of hand gesture such as basic finger movements, basic wrist movements, and grasp and functional movements. In our

work, the proposed approach was evaluated on 4 subdatabases of the NinaPro database (denoted as NinaPro DB2, NinaPro DB3, NinaPro DB5, NinaPro DB7) [28-30]. As shown in Table I, all these databases comprise sEMG signals and the corresponding ACC signals sensed by IMU. Referring to the experimental

setup of Wei et al. [20], we excluded subject data from the aforementioned databases that lacked complete channel and action information.

2) *SIEM database*: SIEM database is a hybrid sEMG signal database presented by Hu et al [69], comprising 20 able-bodied subjects performed 12 finger movements under two paces and three arm postures. The database contains HD-sEMG signals recorded with a 64-channel high-density grid placed on the back of hand, sparse 8-channel sEMG signals and 3-channel IMU signals (Euler angles) recorded by a Myo armband around the forearm, all at a sampling rate of 2040Hz. Consistent with the FEMG-VPF dataset, the sparse 8-channel sEMG signal and corresponding 3-channel Euler angles gathered by the Myo armband used in this work. The signal recorded in three experiment sessions, and in each session, a subject was required to complete three fast and three slow trials in turn under different arm postures. To eliminate the potential impact of inter-session variations on the experimental results, we choose data from a single session for comparative validation.

### C. Signal Processing

Root Mean Square (RMS) of SEMG is related to the number of active muscle fibers, the rate of activation and the isometric contraction force of the muscle in a short time [75]. Compared to rectified sEMG signals, using the RMS filter can effectively minimise amplitude cancelation in the signal [76]. Therefore, a moving RMS filter of 100 milliseconds was performed during GAN model training to obtain low-frequency sEMG activation signals in this work [77]. As the relatively smooth characteristics of IMU signals (ACC signals and Euler angle signals in this work) compared to sEMG signals, and to avoid introducing excessive computational complexity, a moving average filter of 100 milliseconds was performed on raw IMU signals during GAN model training to ensure that the sample size of IMU signals aligns with that of sEMG signals [78, 79]. In addition, we filter the absolute value of the raw sEMG signals of each electrode separately with a first-order low-pass Butterworth filter (with a cut-off frequency of 1 Hz) in HGR experiments. Due to memory limitations, for the HGR experiments on FEMG-VPF Database, NinaPro DB2, DB3, DB7 and SIEM Database we performed a

downsampling process by a factor of 20 on both the sEMG signals and the generated virtual IMU signals, respectively [20, 69]. To ensure real-time control, input delay was a crucial factor to be considered. A classical study suggested that the maximum allowable delay is 300 milliseconds [80]. For comparison with prior work, a slide window size of 200 milliseconds and step of 10 milliseconds was considered for segmentation of the sEMG signals and generated virtual IMU signals.

### D. Experimental Setup

The proposed generative multimodal HGR approach was conducted using the TensorFlow 2.0 framework, implemented in Python. Data preprocessing and model training were performed on an AMAX TD21-Z2 workstation with the following hardware configuration: Ubuntu 20.04 operating system, 128 GB of RAM, Intel I9 10900X processor, and two NVIDIA GeForce GTX3080Ti graphics cards.

The proposed GAN-based deep generative model was trained using the Adaptive Moment Estimation (Adam) algorithm with a learning rate of 0.0002 and batch size of 64. The total number of training epochs was set to 10000. The dropout was set to 0.2 in the discriminator. The multimodal CNN was trained using Stochastic Gradient Descent (SGD) with a batch size of 64 and epoch of 28. To accelerate convergence, a learning rate decay strategy was adopted, with an initial learning rate of 0.1 and divided by 10 after the 16th and 24th epochs. To ensure sufficient training samples, the training sets of all subjects were used for pretraining, and for each subject, the CNN was initialized by the pretrained model. The dropout was set to 0.5 during the pretraining stage.

There were two experiments in this work, both of which are performed on the our collected FEMG-VPF database, Ninapro DB2, DB3, DB5, DB7 and SIEM database. Specifications of the two experiments listed in Table III. As shown in Table III, the data from half of the subjects was utilized to train the GAN model, while the data from the remaining subjects was used for gesture recognition in Experiment 1. Gesture recognition in Experiment 1 is conducted on only half of the subjects' data, rendering the results incomparable with previous work. To address this issue, the gesture recognition training data from all subjects was utilized to train the

GAN model, then the data from all subjects was used for gesture recognition testing in Experiment 2.

TABLE III  
SPECIFICATIONS OF THE TWO EXPERIMENTS USED IN THIS PAPER

	Databases	GAN model		gesture recognition		
		Number of subjects	Trials for training	Number of subjects	Trials for training	Trials for testing
Experiment 1	FEMG-VPF Database	14	1, 2, 3, 4	14	1, 3	2, 4
	NinaPro DB2 [28]	20	1, 2, 3, 4, 5, 6	20	1, 3, 4, 6	2, 5
	NinaPro DB3 [28]	3	1, 2, 3, 4, 5, 6	3	1, 3, 4, 6	2, 5
	NinaPro DB5 [29]	5	1, 2, 3, 4, 5, 6	5	1, 3, 4, 6	2, 5
	NinaPro DB7 [30]	10	1, 2, 3, 4, 5, 6	10	1, 3, 4, 6	2, 5
	SIEM Database [69]	10	1, 2, 3, 4, 5, 6	10	1, 3, 4, 6	2, 5
Experiment 2	FEMG-VPF Database	28	1, 3	28	1, 3	2, 4
	NinaPro DB2 [28]	40	1, 3, 4, 6	40	1, 3, 4, 6	2, 5
	NinaPro DB3 [28]	6	1, 3, 4, 6	6	1, 3, 4, 6	2, 5
	NinaPro DB5 [29]	10	1, 3, 4, 6	10	1, 3, 4, 6	2, 5
	NinaPro DB7 [30]	20	1, 3, 4, 6	20	1, 3, 4, 6	2, 5
	SIEM Database [69]	20	1, 3, 4, 6	20	1, 3, 4, 6	2, 5

#### A. Evaluation of the Proposed Generative Multimodal HGR Approach

In this subsection, we present the evaluations conducted to validate the effectiveness of our proposed generative multimodal HGR approach. We compared the gesture recognition performance achieved by the proposed generative multimodal HGR approach using sEMG signals and generated virtual IMU signals with the unimodal HGR approach only using sEMG signals. The sEMG-based unimodal HGR utilizes a unimodal CNN model, which is a single stream submodel of multimodal CNN model proposed in this work.

The gesture recognition accuracies achieved by the proposed generative multimodal HGR approach and unimodal HGR approach are shown in Fig. 7. The generative multimodal HGR approach achieved higher gesture recognition accuracy than did unimodal HGR approach. For Experiment 1, the proposed approach achieves 69.67%, 87.79%, 80.13%, 94.05%, 95.06% and 72.24% accuracy on FEMG-VPF, DB2, DB3, DB5, DB7 and SIEM database, which is 6.74%, 10.58%, 11.43%, 2.15%, 5.25% and 3.27% higher than that of unimodal HGR approach, respectively. For Experiment 2, the proposed approach achieves 70.06%, 88.31%, 74.35%, 94.18%, 93.53% and 73.21% accuracy on FEMG-VPF, DB2, DB3, DB5, DB7 and SIEM database,

which is 7.90%, 10.37%, 13.10%, 2.37%, 3.41% and 4.19% higher than that of unimodal HGR approach, respectively.

For DB2, DB3, DB5 and DB7, the incorporation of virtual ACC signals resulted in an accuracy improvement of a maximum 13.10%. The accuracy improvement for DB5 was limited, which can be attributed to 1) the higher baseline accuracy of DB5 (exceeding 90.00%), making further improvement challenging; 2) DB5 incorporated 3-channel virtual ACC signals, whereas the other databases utilized 36-channel virtual ACC signals. For the FEMG-VPF and SIEM databases, we incorporated 3-channel virtual Euler angle signals. The FEMG-VPF database exhibited lower baseline results, which might be attributed to the quality of our database. To better simulate real-world scenarios, we did not rigorously abrade the skin and apply conductive gel during data acquisition, which might have introduced more noise [81]. Nonetheless, with incorporating the virtual Euler angle signals, a significant improvement in the results was observed (an increase of 6.74% and 7.90% respectively). Overall, the experiment results indicates that incorporating virtual IMU signals, whether ACC or Euler angles, can significantly improve the accuracy of sEMG-based HGR.

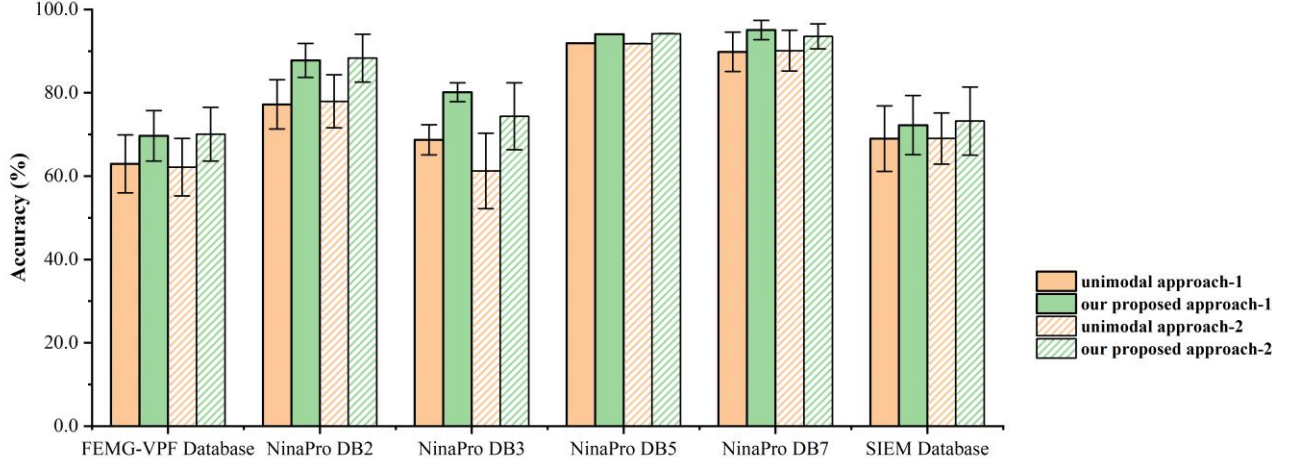


Fig. 7. Performance comparison of the our proposed generative multimodal HGR approach and unimodal HGR approach. 1 and 2 in the legend represent Experiment 1 and Experiment 2, respectively. The height of each column represents the average accuracy, while the error bars represent the standard deviation

#### B. Comparison With the State-of-the-Art Gesture Recognition Approaches

This subsection presents a performance comparison with state-of-the-art sEMG-based gesture recognition approaches to demonstrate the advantages of our proposed generative multimodal HGR approach. This comparison was conducted on 4 subdatabases of NinaPro. The specifications of these databases and the experimental setups used these databases are described in Sections V-B and V-D. The gesture recognition accuracy of our proposed approach used here is the result on the Experiment 2. The experimental results reported in previous studies as well as those achieved by our proposed generative multimodal HGR approach on the evaluated sEMG databases are summarized in Table IV. To ensure consistency among subjects, the result

from DB3 were solely compared to the result of MV-CNN [20], and the result from DB7 were compared to the result obtained from the 20 able-bodied subjects. As shown in Table IV, the gesture recognition accuracies achieved by proposed approach on different sEMG databases surpass those attained by the state-of-the-art methods, even though some methods focused on classifying fewer gestures or adopted longer windows. Moreover, our proposed approach directly utilizes raw sEMG signals for gesture recognition, instead of performing feature extraction on sEMG signals, as done in methods like MV-CNN [20]. Thus, our proposed approach also offers advantages such as reduced computational load and storage requirements. The trade-off between accuracy and computation is more suitable and compact for real-time application [82].

TABLE IV  
GESTURE RECOGNITION ACCURACIES OF THE PROPOSED APPROACH COMPARED WITH THE ACCURACIES OF EXISTING WORKS ON 4 SEMG DATABASES.

THE BOLD ENTRIES INDICATE THE SCORES OF THE PROPOSED APPROACH

Database	Method	number of subject	number of gestures	window length ( ms)	Accuracy ( %)
NinaPro DB2	Random Forest [28]	40	50	200	75.27
	ZhaiNet [83]	40	50	200	78.71
	HuNet [84]	40	50	200	82.20
	MV-CNN [20]	40	50	200	83.70
	TC-HGR [85]	40	50	200	80.72
	Our proposed approach	40	50	200	<b>88.31</b>
NinaPro DB3	MV -CNN [20]	6	50	200	64.30
	Our proposed approach	6	50	200	<b>74.35</b>
NinaPro DB5	SVM [29]	10	41	200	69.04
	MV-CNN [20]	10	41	200	90.00
	ShenNet [39]	10	52	200	74.51
	Alexnet [86]	10	53	250	70.40
	LiNet [87]	10	52	500	90.82
	Our proposed approach	10	53	200	<b>94.18</b>
NinaPro DB7	LDA [30]	20	40	256	60.10
	MV-CNN [20]	20	41	200	88.30
	DNN [88]	20	41	200	85.08
	MMDF [89]	20	40	256	91.40
	Our proposed approach	20	41	200	<b>93.53</b>

## VI. CONCLUSION

Multimodal gesture recognition technology is an effective means to improve the accuracy in recognizing gestures composed of hand and forearm movements, but it often results in increased hardware costs. To address this issue, we proposed a novel approach to improve sEMG-based HGR accuracy via virtual IMU signals. The virtual IMU signals was generated by a trained GAN-based deep generative model from the input sEMG signals and subsequently the sEMG signals and virtual IMU signals were fed into a multimodal CNN model for gesture recognition. Evaluations on 5 public databases and our collected database demonstrated that the proposed approach achieved higher gesture recognition accuracies than those achieved by sEMG-based unimodal HGR method. Compared with the

sEMG-based unimodal HGR method, the recognition accuracy of the proposed approach was increased by %-% on FEMG-VPF database, NinaPro DB2, DB3, DB5, DB7 and SIEM database, which indicated that incorporating virtual IMU signals can significantly improve the accuracy of sEMG-based HGR.

There are certain limitations that should be considered in future work. This study is a preliminary exploration that using generative models to bridge the gap between the unimodal HGR and multimodal HGR without additional sensor hardware. We adopted a relatively simple GAN model to generate the additional modalities. Specifically, we focused on generating ACC signals and Euler angle signals. The simplicity of the GAN model used in this work may lead to limited expressive power and less fine-grained generation of signals. Nonetheless,

our proposed approach demonstrated the feasibility of improving gesture recognition accuracy through generative models. Our future work will focus on incorporating new data modalities to further improve the accuracy of the proposed approach using the latest generative models, such as VAE and Diffusion Model. We will also attempt to generate of finger joint angles directly, thus escaping the limitation of gesture types. This will bring more natural and convenient interaction experience in medical rehabilitation, smart home, virtual reality and other fields, and is of great significance for promoting the further development and application of low-cost human-computer interaction technology.

## REFERENCES

- [1] C. Shen, Z. Pei, W. Chen, J. Wang, J. Zhang, and Z. Chen, "Toward Generalization of sEMG-Based Pattern Recognition: A Novel Feature Extraction for Gesture Recognition," *IEEE Trans. Instrum. Meas.*, vol. 71, pp. 1-12, Jan. 2022, doi: 10.1109/TIM.2022.3141163.
- [2] L. Guo, Z. Lu, and L. Yao, "Human-Machine Interaction Sensing Technology Based on Hand Gesture Recognition: A Review," *IEEE Trans. Hum.-Mach. Syst.*, vol. 51, no. 4, pp. 300-309, Aug. 2021, doi: 10.1109/THMS.2021.3086003.
- [3] W. Wei, Y. Wong, Y. Du, Y. Hu, M. Kankanhalli, and W. Geng, "A multi-stream convolutional neural network for sEMG-based gesture recognition in muscle-computer interface," *Pattern Recognit. Lett.*, vol. 119, pp. 131-138, Mar. 2019, doi: 10.1016/j.patrec.2017.12.005.
- [4] B. Fang *et al.*, "Simultaneous sEMG Recognition of Gestures and Force Levels for Interaction With Prosthetic Hand," *IEEE Trans. Neural Syst. Rehabil. Eng.*, vol. 30, pp. 2426-2436, 2022, doi: 10.1109/TNSRE.2022.3199809.
- [5] J. Xue, Z. Sun, F. Duan, C. F. Caiafa, and J. Solé-Casals, "Underwater sEMG-based recognition of hand gestures using tensor decomposition," *Pattern Recognit. Lett.*, vol. 165, pp. 39-46, Jan. 2023, doi: 10.1016/j.patrec.2022.11.021.
- [6] X. Song, S. S. Van De Ven, L. Liu, F. J. Wouda, H. Wang, and P. B. Shull, "Activities of Daily Living-Based Rehabilitation System for Arm and Hand Motor Function Retraining After Stroke," *IEEE Trans. Neural Syst. Rehabil. Eng.*, vol. 30, pp. 621-631, Mar. 2022, doi: 10.1109/TNSRE.2022.3156387.
- [7] F. Xiao, Z. Zhang, C. Liu, and Y. Wang, "Human motion intention recognition method with visual, audio, and surface electromyography modalities for a mechanical hand in different environments," *Biomed. Signal Process. Control*, vol. 79, p. 104089, Jan. 2023, doi: 10.1016/j.bspc.2022.104089.
- [8] K. A. Shatilov, Y. D. Kwon, L. H. Lee, D. Chatzopoulos, and P. Hui, "MyoKey: Inertial Motion Sensing and Gesture-based QWERTY Keyboard for Extended Realities," *IEEE Trans. Mobile Comput.*, Aug. 2023, doi: 10.1109/TMC.2022.3156939.
- [9] U. Côté-Allard *et al.*, "A Transferable Adaptive Domain Adversarial Neural Network for Virtual Reality Augmented EMG-Based Gesture Recognition," *IEEE Trans. Neural Syst. Rehabil. Eng.*, vol. 29, pp. 546-555, 2021, doi: 10.1109/TNSRE.2021.3059741.
- [10] J. Xue and K. W. C. Lai, "Dynamic gripping force estimation and reconstruction in EMG-based human-machine interaction," *Biomed. Signal Process. Control*, vol. 80, p. 104216, Feb. 2023, doi: 10.1016/j.bspc.2022.104216.
- [11] M. F. Qureshi, Z. Mushtaq, M. Z. u. Rehman, and E. N. Kamavuako, "Spectral Image-Based Multiday Surface Electromyography Classification of Hand Motions Using CNN for Human-Computer Interaction," *IEEE Sensors J.*, vol. 22, no. 21, pp. 20676-20683, Nov. 2022, doi: 10.1109/JSEN.2022.3204121.
- [12] S. Ahmed, W. Kim, J. Park, and S. H. Cho, "Radar-Based Air-Writing Gesture Recognition Using a Novel Multistream CNN Approach," *IEEE Internet Things J.*, vol. 9, no. 23, pp. 23869-23880, Dec. 2022, doi: 10.1109/JIOT.2022.3189395.
- [13] K. Lu *et al.*, "Channel-distribution Hybrid Deep Learning for sEMG-based Gesture Recognition," in *Proc. IEEE Int. Conf. Robot. Biomimetics*, Jinghong, China, 2022, pp. 278-284: .
- [14] Y. Fang, J. Yang, D. Zhou, and Z. Ju, "Modelling EMG driven wrist movements using a bio-inspired neural network," *Neurocomputing*, vol. 470, pp. 89-98, Jan. 2022, doi: 10.1016/j.neucom.2021.10.104.
- [15] Y. Lin, R. Palaniappan, P. De Wilde, and L. Li, "Reliability Analysis for Finger Movement Recognition With Raw Electromyographic Signal by Evidential Convolutional Networks," *IEEE Trans. Neural Syst. Rehabil. Eng.*, vol. 30, pp. 96-107, Jan. 2022, doi: 10.1109/TNSRE.2022.3141593.
- [16] D. Vera Anaya and M. R. Yuce, "Stretchable triboelectric sensor for measurement of the forearm muscles movements and fingers motion for Parkinson's disease assessment and assisting technologies," *Med. Devices Sens.*, vol. 4, no. 1, p. e10154, Feb. 2021, doi: 10.1002/mds3.10154.
- [17] N. Akhlaghi *et al.*, "Real-Time Classification of Hand Motions Using Ultrasound Imaging of Forearm Muscles," *IEEE Trans. Biomed. Eng.*, vol. 63, no. 8, pp. 1687-1698, Aug. 2016, doi: 10.1109/TBME.2015.2498124.
- [18] J. Yang, J. Pan, and J. Li, "sEMG-based continuous hand gesture recognition using GMM-HMM and threshold model," in *Proc. IEEE Int. Conf. Robot. Biomimetics*, Macau, Macao., 2017, pp. 1509-1514.
- [19] S. Jiang *et al.*, "Feasibility of Wrist-Worn, Real-Time Hand, and Surface Gesture Recognition via sEMG and IMU Sensing," *IEEE Trans. Ind. Informat.*, vol. 14, no. 8, pp. 3376-3385, Aug. 2018, doi: 10.1109/TII.2017.2779814.
- [20] W. Wei, Q. Dai, Y. Wong, Y. Hu, M. Kankanhalli, and W. Geng,

- "Surface-Electromyography-Based Gesture Recognition by Multi-View Deep Learning," *IEEE Trans. Biomed. Eng.*, vol. 66, no. 10, pp. 2964-2973, Oct 2019, doi: 10.1109/TBME.2019.2899222.
- [21] S. Duan, L. Wu, B. Xue, A. Liu, R. Qian, and X. Chen, "A Hybrid Multimodal Fusion Framework for sEMG-ACC-Based Hand Gesture Recognition," *IEEE Sensors J.*, vol. 23, no. 3, pp. 2773-2782, Feb. 2023, doi: 10.1109/JSEN.2022.3231925.
- [22] J. Zhang, Q. Wang, Q. Wang, and Z. Zheng, "Multimodal Fusion Framework Based on Statistical Attention and Contrastive Attention for Sign Language Recognition," *IEEE Trans. Mobile Comput.*, 2023, doi: 10.1109/TMC.2023.3235935.
- [23] T. Y. Pan, W. L. Tsai, C. Y. Chang, C. W. Yeh, and M. C. Hu, "A Hierarchical Hand Gesture Recognition Framework for Sports Referee Training-Based EMG and Accelerometer Sensors," *IEEE Trans. Cybern.*, vol. 52, no. 5, pp. 3172-3183, May. 2022, doi: 10.1109/TCYB.2020.3007173.
- [24] J. Wu, L. Sun, and R. Jafari, "A Wearable System for Recognizing American Sign Language in Real-Time Using IMU and Surface EMG Sensors," *IEEE J. Biomed. Health Informat.*, vol. 20, no. 5, pp. 1281-1290, Sep. 2016, doi: 10.1109/JBHI.2016.2598302.
- [25] Y. Hu, Y. Wong, Q. Dai, M. Kankanhalli, W. Geng, and X. Li, "sEMG-Based Gesture Recognition With Embedded Virtual Hand Poses and Adversarial Learning," *IEEE Access*, vol. 7, pp. 104108-104120, 2019, doi: 10.1109/ACCESS.2019.2930005.
- [26] A. Oussidi and A. Elhassouny, "Deep generative models: Survey," in *Proc. Int. Conf. Intell. Syst. Comput. Vis.*, Fez, Morocco, 2018, pp. 1-8.
- [27] I. Goodfellow *et al.*, "Generative adversarial nets," in *Proc. 27th Int. Conf. Neural Inf. Process. Syst.*, Montreal, Quebec, Canada, 2014, pp. 2672-2680.
- [28] M. Atzori *et al.*, "Electromyography data for non-invasive naturally-controlled robotic hand prostheses," *Sci. Data*, vol. 1, no. 1, Dec. 2014.
- [29] S. Pizzolato, L. Tagliapietra, M. Cognolato, M. Reggiani, H. Müller, and M. Atzori, "Comparison of six electromyography acquisition setups on hand movement classification tasks," *PLoS ONE*, vol. 12, no. 10, p. e0186132, 2017, doi: 10.1371/journal.pone.0186132.
- [30] A. Krasoulis, I. Kyranou, M. S. Erden, K. Nazarpour, and S. Vijayakumar, "Improved prosthetic hand control with concurrent use of myoelectric and inertial measurements," *J. Neuroeng. Rehabil.*, vol. 14, pp. 1-14, Jul. 2017, doi: 10.1186/s12984-017-0284-4.
- [31] F. Palermo, M. Cognolato, A. Gijsberts, H. Müller, B. Caputo, and M. Atzori, "Repeatability of grasp recognition for robotic hand prosthesis control based on sEMG data," *Proc. IEEE Int. Conf. Rehabil. Robot.*, pp. 1154-1159, 2017, doi: 10.1109/ICORR.2017.8009405.
- [32] A. Krasoulis, S. Vijayakumar, and K. Nazarpour, "Effect of user practice on prosthetic finger control with an intuitive myoelectric decoder," *Frontiers Neurosci.*, vol. 13, p. 891, Sep. 2019, doi: 10.3389/fnins.2019.00891.
- [33] X. Jiang *et al.*, "Optimization of HD-sEMG-Based Cross-Day Hand Gesture Classification by Optimal Feature Extraction and Data Augmentation," *IEEE Trans. Hum.-Mach. Syst.*, vol. 52, no. 6, pp. 1281-1291, Dec. 2022, doi: 10.1109/THMS.2022.3175408.
- [34] E. Tyacke *et al.*, "Hand Gesture Recognition via Transient sEMG Using Transfer Learning of Dilated Efficient CapsNet: Towards Generalization for Neurorobotics," *IEEE Robot. Autom. Lett.*, vol. 7, no. 4, pp. 9216-9223, 2022, doi: 10.1109/LRA.2022.3191238.
- [35] S. Wei, Z. Y., and H. Liu, "A Multimodal Multilevel Converged Attention Network for Hand Gesture Recognition With Hybrid sEMG and A-Mode Ultrasound Sensing," *IEEE Trans. Cybern.*, 2022, doi: 10.1109/TCYB.2022.3204343.
- [36] Y. Yang *et al.*, "Performance Comparison of Gesture Recognition System Based on Different Classifiers," *IEEE Trans. Cognit. Develop. Syst.*, vol. 13, no. 1, pp. 141-150, Mar. 2021, doi: 10.1109/tcds.2020.2969297.
- [37] A. Fatayer, W. Gao, and Y. Fu, "sEMG-Based Gesture Recognition Using Deep Learning From Noisy Labels," *IEEE J. Biomed. Health Informat.*, vol. 26, no. 9, pp. 4462-4473, Sep. 2022, doi: 10.1109/JBHI.2022.3179630.
- [38] Y. Zhang, F. Yang, Q. Fan, A. Yang, and X. Li, "Research on sEMG-Based Gesture Recognition by Dual-View Deep Learning," *IEEE Access*, vol. 10, pp. 32928-32937, 2022, doi: 10.1109/ACCESS.2022.3158667.
- [39] S. Shen, K. Gu, X. R. Chen, C. X. Lv, and R. C. Wang, "Gesture Recognition Through sEMG with Wearable Device Based on Deep Learning," *Mobile Netw. Appl.*, vol. 25, pp. 2447-2458, Jul. 2020, doi: 10.1007/s11036-020-01590-8.
- [40] W. Geng, Y. Du, W. Jin, W. Wei, Y. Hu, and J. Li, "Gesture recognition by instantaneous surface EMG images," *Sci. Rep.*, vol. 6, p. 36571, Nov. 2016.
- [41] S. Shen, X. Wang, F. Mao, L. Sun, and M. Gu, "Movements Classification Through sEMG With Convolutional Vision Transformer and Stacking Ensemble Learning," *IEEE Sensors J.*, vol. 22, no. 13, pp. 13318-13325, Jul. 2022, doi: 10.1109/JSEN.2022.3179535.
- [42] H. Wang, Y. Zhang, C. Liu, and H. Liu, "sEMG based hand gesture recognition with deformable convolutional network," *Int. J. Mach. Learn. Cybern.*, vol. 13, no. 6, pp. 1729-1738, Jan. 2022, doi: 10.1007/s13042-021-01482-7.
- [43] Y. Liu, X. Li, L. Yang, G. Bian, and H. Yu, "A CNN-Transformer Hybrid Recognition Approach for sEMG-based Dynamic Gesture Prediction," *IEEE Trans. Instrum. Meas.*, vol. 72, pp. 1-16, 2023, doi: 10.1109/TIM.2023.3273651.



- [44] Ctrl-Labs: <https://www.ctrl-labs.com/>.
- [45] eCon: [torintek.com/wearables](http://torintek.com/wearables).
- [46] S. Shen, X. Wang, M. Wu, K. Gu, X. Chen, and X. Geng, "ICA-CNN: Gesture Recognition Using CNN With Improved Channel Attention Mechanism and Multimodal Signals," *IEEE Sensors J.*, vol. 23, no. 4, pp. 4052-4059, Feb. 2023, doi: 10.1109/JSEN.2023.3236682.
- [47] M. Kahng, N. Thorat, D. H. Chau, F. B. Viégas, and M. Wattenberg, "GAN Lab: Understanding Complex Deep Generative Models using Interactive Visual Experimentation," *IEEE Trans. Visualization Comput. Graph.*, vol. 25, no. 1, pp. 310-320, Jan. 2019, doi: 10.1109/TVCG.2018.2864500.
- [48] M. Mirza and S. Osindero, "Conditional generative adversarial nets," 2014, arXiv:1411.1784.
- [49] A. Radford, L. Metz, and S. Chintala, "Unsupervised representation learning with deep convolutional generative adversarial networks," 2015, arXiv:1511.06434.
- [50] M. Arjovsky, S. Chintala, and L. Bottou, "Wasserstein GAN," 2017, arXiv:1701.07875.
- [51] D. P. Kingma and M. Welling, "Auto-encoding variational bayes," 2013, arXiv:1312.6114.
- [52] J. Ho, J. A., and P. Abbeel, "Denoising diffusion probabilistic models," in *Proc. 33rd Int. Conf. Neural Inf. Process. Syst.*, 2020, pp. 6840-6851.
- [53] S. Lee, H. Chung, J. Kim, and J. C. Ye, "Progressive deblurring of diffusion models for coarse-to-fine image synthesis," 2022, arXiv:2207.11192.
- [54] D. Chira, I. Haralampiev, O. Winther, A. Dittadi, and V. Liévin, "Image Super-Resolution with Deep Variational Autoencoders," presented at the Computer Vision – ECCV 2022 Workshops, 2023.
- [55] W. Ahmad, H. Ali, Z. Shah, and S. Azmat, "A new generative adversarial network for medical images super resolution," *Sci. Rep.*, vol. 9533, Jun. 2022, doi: 10.1038/s41598-022-13658-4.
- [56] S. Gong, M. Li, J. Feng, Z. Wu, and L. Kong, "Diffuseq: Sequence to sequence text generation with diffusion models," 2022, arXiv:2210.08933.
- [57] Z. Kong, W. Ping, Huang, J. K. Zhao, and B. Catanzaro, "Diffwave: A versatile diffusion model for audio synthesis," 2020, arXiv:2009.09761.
- [58] R. Huang *et al.*, "Make-an-audio: Text-to-audio generation with prompt-enhanced diffusion models," 2023, arXiv:2301.12661.
- [59] Y. Xue, Y. Yu, K. Yin, P. Li, S. Xie, and Z. Ju, "Human In-Hand Motion Recognition Based on Multi-Modal Perception Information Fusion," *IEEE Sensors J.*, vol. 22, no. 7, pp. 6793-6805, Apr. 2022, doi: 10.1109/JSEN.2022.3148992.
- [60] L. J. Ratliff, S. A. Burden, and S. S. Sastry, "Characterization and computation of local Nash equilibria in continuous games," in *Proc. Annu. Allerton Conf. Commun. Control Comput.*, Monticello, IL, USA, 2013, pp. 917-924.
- [61] K. Wang, C. Gou, Y. Duan, Y. Lin, Z. X., and F. Wang, "Generative adversarial networks: introduction and outlook," *IEEE/CAA J. Automatica Sinica*, vol. 4, no. 5, pp. 588-598, 2017, doi: 10.1109/JAS.2017.7510583.
- [62] W. Fang, Y. Ding, F. Zhang, and J. Sheng, "Gesture Recognition Based on CNN and DCGAN for Calculation and Text Output," *IEEE Access*, vol. 7, pp. 28230-28237, 2019, doi: 10.1109/ACCESS.2019.2901930.
- [63] S. Ioffe and C. Szegedy, "Batch Normalization: Accelerating Deep Network Training by Reducing Internal Covariate Shift," in *Proc. Int. Conf. Mach. Learn.*, New York, N. Y. USA, 2015, pp. 448-456: ACM.
- [64] X. Glorot, A. Bordes, and Y. Bengio, "Deep sparse rectifier neural networks," in *Proc. 14th Int. Conf. Artif. Intell. Statist.*, 2011, vol. 15, pp. 315-323.
- [65] J. Xu, Z. Li, B. Du, M. Zhang, and J. Liu, "Reluplex made more practical: Leaky ReLU," in *Proc. IEEE Symp. Comput. Commun.*, Rennes, France, 2020, pp. 1-7.
- [66] N. Srivastava, G. Hinton, A. Krizhevsky, I. Sutskever, and R. Salakhutdinov, "Dropout: A Simple Way to Prevent Neural Networks from Overfitting," *J. Mach. Learn. Res.*, vol. 15, pp. 1929-1958, 2014.
- [67] D. J. Saunders, D. Patel, H. Hazan, H. T. Siegelmann, and R. Kozma, "Locally connected spiking neural networks for unsupervised feature learning," *Neural Netw.*, vol. 119, pp. 332-340, Nov. 2019, doi: 10.1016/j.neunet.2019.08.016.
- [68] H. Ci, X. Ma, C. Wang, and Y. Wang, "Locally Connected Network for Monocular 3D Human Pose Estimation," *IEEE Trans. Pattern Anal. Mach. Intell.*, vol. 44, no. 3, pp. 1429-1442, Mar. 2022, doi: 10.1109/TPAMI.2020.3019139.
- [69] X. Hu, A. Song, J. Wang, H. Zeng, and W. Wei, "Finger Movement Recognition via High-Density Electromyography of Intrinsic and Extrinsic Hand Muscles," *Sci. Data*, vol. 9, no. 1, p. 373, Jun. 2022, doi: 10.1038/s41597-022-01484-2.
- [70] S. Tanzarella, S. Muceli, A. Del Vecchio, A. Casolo, and D. Farina, "Non-invasive analysis of motor neurons controlling the intrinsic and extrinsic muscles of the hand," *J. Neural Eng.*, vol. 17, p. 046033, Aug. 2020, doi: 10.1088/1741-2552/aba6db.
- [71] U. Côté-Allard, C. L. Fall, A. Campeau-Lecours, and C. Go, "Transfer learning for sEMG hand gestures recognition using convolutional neural networks," in *Proc. IEEE Int. Conf. Syst. Man Cybern.*, Banff, AB, Canada, 2017, no. 1663-1668.
- [72] J. L. Betthausen *et al.*, "Stable Responsive EMG Sequence Prediction and Adaptive Reinforcement With Temporal Convolutional Networks," *IEEE Trans. Biomed. Eng.*, vol. 67, no. 6, pp. 1707-1717, Jun. 2020, doi: 10.1109/TBME.2019.2943309.
- [73] L. E. Osborn *et al.*, "Extended home use of an advanced

- osseointegrated prosthetic arm improves function, performance, and control efficiency," *J. Neural Eng.*, vol. 18, no. 2, Mar. 2021, doi: 10.1088/1741-2552/abe20d.
- [74] L. Ren and W. Wei, "Forearm Gesture Dataset: Gesture Recognition under Different Arm Postures and Force Levels," *figshare. Dataset*, Aug. 2023, doi: 10.6084/m9.figshare.23850366.v1.
- [75] L. Xu, K. Zhang, G. Yang, and J. Chu, "Gesture recognition using dual-stream CNN based on fusion of sEMG energy kernel phase portrait and IMU amplitude image," *Biomed. Signal Process. Control*, vol. 73, p. 103364, Mar. 2022, doi: 10.1016/j.bspc.2021.103364.
- [76] G. S. Trajano, K. Nosaka, and A. J. Blazevich, "Neurophysiological Mechanisms Underpinning Stretch-Induced Force Loss," *Sports Med.*, vol. 47, pp. 1531–1541, Jan. 2017, doi: 10.1007/s40279-017-0682-6.
- [77] Y. Yang, J. Ren, and F. Duan, "The Spiking Rates Inspired Encoder and Decoder for Spiking Neural Networks: An Illustration of Hand Gesture Recognition," *Cognitive Computation*, May. 2022, doi: 10.1007/s12559-022-10027-1.
- [78] Z. Lu, X. Chen, Q. Li, X. Zhang, and P. Zhou, "A Hand Gesture Recognition Framework and Wearable Gesture-Based Interaction Prototype for Mobile Devices," *IEEE Trans. Hum.-Mach. Syst.*, vol. 44, no. 2, pp. 293-299, Apr. 2014, doi: 10.1109/THMS.2014.2302794.
- [79] Y. L. Hsu, C. L. Chu, Y. J. Tsai, and J. S. Wang, "An Inertial Pen With Dynamic Time Warping Recognizer for Handwriting and Gesture Recognition," *IEEE Sensors J.*, vol. 15, no. 1, pp. 154-163, Jan. 2015, doi: 10.1109/JSEN.2014.2339843.
- [80] B. Hudgins, P. Parker, and R. N. Scott, "A new strategy for multifunction myoelectric control," *IEEE Trans. Biomed. Eng.*, vol. 40, no. 1, pp. 82-94, Jan. 1993, doi: 10.1109/10.204774.
- [81] L. Tian *et al.*, "Large-area MRI-compatible epidermal electronic interfaces for prosthetic control and cognitive monitoring," *Nat. Biomed. Eng.*, vol. 3, no. 3, pp. 194-205, Feb. 2019, doi: 10.1038/s41551-019-0347-x.
- [82] C. Xu, X. Wu, M. Wang, F. Qiu, Y. Liu, and J. Ren, "Improving dynamic gesture recognition in untrimmed videos by an online lightweight framework and a new gesture dataset ZJUGesture," *Neurocomputing*, vol. 528, pp. 58-68, Feb. 2023, doi: 10.1016/j.neucom.2022.12.022.
- [83] X. Zhai, B. Jelfs, R. H. M. Chan, and C. Tin, "Self-Recalibrating Surface EMG Pattern Recognition for Neuroprosthesis Control Based on Convolutional Neural Network," *Frontiers Neurosci.*, vol. 11, p. 379, Jul. 2017, doi: 10.3389/fnins.2017.00379.
- [84] Y. Hu, Y. Wong, W. Wei, Y. Du, M. Kankanhalli, and W. Geng, "A novel attention-based hybrid CNN-RNN architecture for sEMG-based gesture recognition," *PLoS ONE*, vol. 13, no. 10, p. e0206049, 2018, doi: 10.1371/journal.pone.0206049.
- [85] E. Rahimian, S. Zabihi, A. Asif, D. Farina, S. F. Atashzar, and A. Mohammadi, "Hand Gesture Recognition Using Temporal Convolutions and Attention Mechanism," in *IEEE International Conference on Acoustics, Speech and Signal Processing*, Singapore, 2022, pp. 1196-1200.
- [86] Y. Li, W. Zhang, Q. Zhang, and N. Zheng, "Transfer Learning-Based Muscle Activity Decoding Scheme by Low-frequency sEMG for Wearable Low-cost Application," *IEEE Access*, vol. 9, pp. 22804-22815, 2021, doi: 10.1109/ACCESS.2021.3056412.
- [87] Y. Li, J. Li, P. Tu, H. Wang, and K. Wang, "Gesture Recognition Based on EEMD and Cosine Laplacian Eigenmap," *IEEE Sensors J.*, vol. 23, no. 14, pp. 16332-16342, Jul. 2023, doi: 10.1109/JSEN.2023.3279555.
- [88] P. Sri-Iesaranusorn *et al.*, "Classification of 41 Hand and Wrist Movements via Surface Electromyogram Using Deep Neural Network," *Frontiers Bioeng. Biotechnol.*, vol. 9, p. 548357, Jun. 2021, doi: 10.3389/fbioe.2021.548357.
- [89] Y. Fang, H. Lu, and H. Liu, "Multi-modality deep forest for hand motion recognition via fusing sEMG and acceleration signals," *Int. J. Mach. Learn. Cybern.*, Nov. 2022, doi: 10.1007/s13042-022-01687-4.